Hydrogen peroxide alters membrane and cytoskeleton properties and increases intercellular connections in astrocytes

Donghui Zhu[1], Kevin S. Tan[2], Xiaolin Zhang[2], Albert Y. Sun[3], Grace Y. Sun[2] and James C.-M. Lee[1,*]

[1]Department of Biological Engineering, [2]Department of Biochemistry, and [3]Department of Pharmacology and Physiology, University of Missouri-Columbia, Columbia, MO 65211, USA

*Author for correspondence (e-mail: Leejam@missouri.edu)

Accepted 23 May 2005
Journal of Cell Science 118, 3695-3703 Published by The Company of Biologists 2005
doi:10.1242/jcs.02507

Summary

Excess hydrogen peroxide (H_2O_2) is produced in the pathogenesis of brain injuries and neurodegenerative diseases. H_2O_2 may damage cells through direct oxidation of lipids, proteins and DNA or it can act as a signaling molecule to trigger intracellular pathways leading to cell death. In this study, H_2O_2 caused plasma membranes of primary astrocytes to become more gel-like, while artificial membranes of vesicles composed of rat brain lipid extract became more liquid crystalline-like. Besides the effects on membrane phase properties, H_2O_2 promoted actin polymerization, induced the formation of cell-to-cell tunneling nanotube (TNT)-like connections among astrocytes and increased the colocalization of myosin Va with F-actin. Myosin Va was also observed in the H_2O_2-induced F-actin-enriched TNT-like connections. Western blot analysis suggests that H_2O_2 triggered the phosphorylation of the p38 mitogen-activated protein kinase (MAPK), and that SB203580, a specific inhibitor of p38 MAPK, suppressed the changes in membrane phase properties and cytoskeleton resulting from H_2O_2 treatment. These results suggest that H_2O_2 alters astrocyte membranes and the cytoskeleton through activation of the p38 MAPK pathway.

Supplementary material available online at
http://jcs.biologists.org/cgi/content/full/118/16/3695/DC1

Key words: actin, cytoneme, nanotube, oxidative stress, p38 MAPK

Introduction

Owing to their high consumption of oxygen and enrichment of polyunsaturated fatty acids in their membranes, cells in the central nervous system (CNS) are highly susceptible to oxidative damage. Oxidative stress induced by excess production of reactive oxygen species (ROS) has been implicated in pathologic processes associated with brain injuries and other neurodegenerative diseases (Coyle and Puttfarcken, 1993). H_2O_2, a major form of ROS, has been shown to mediate cell damage either through direct oxidation of lipids, proteins and DNA or acting as a signaling molecule to trigger cellular apoptotic pathways (Butterfield and Lauderback, 2002; Howe et al., 2004; Huang et al., 2004; Lin et al., 2004; Shin et al., 2004; van Rossum et al., 2004). Although neurons are generally more susceptible to oxidative injury than astrocytes, it is clear that oxidative stress also alters astrocyte functions (Robb and Connor, 1998). Astrocytes are known to provide vital functions necessary for proper neural performances, including maintenance of ion gradients, metabolism of neurotransmitters, and protecting neurons from oxidative injury (Desagher et al., 1996). Therefore, it is important to understand how oxidative stress alters astrocyte functions.

Lipid peroxidation is associated with modifications of membrane proteins (e.g. receptors, ion transporters and channels) leading to altered Ca^{2+} homeostasis, and Ca^{2+}-dependent kinases (proteases, phospholipases and nucleases), leading to mitochondrial dysfunction and activation of apoptotic pathways (Butterfield and Lauderback, 2002; Gyulkhandanyan et al., 2003; Jacobson and Duchen, 2002; Robb et al., 1999). Despite the metabolic changes, little is known about the direct effects of H_2O_2 on membrane properties of astrocytes. In this study, the effects of H_2O_2 on changes in phase properties of astrocyte membranes were examined by fluorescence spectroscopy of 6-dodecanoyl-2-dimethylaminonaphthalene (Laurdan).

In addition to lipid peroxidation, the cytoskeleton network is also one of the earliest targets of oxidative stress (Dalle-Donne et al., 2001; Zhao and Davis, 1998). There is a growing body of evidence supporting the hypothesis that perturbation of cytoskeletal proteins is the initial step of oxidant-induced cell damage. Although oxidative injury is known to selectively alter cytoskeletal proteins (Aksenov et al., 2001), the mechanism by which oxidants change the structure and the spatial organization of actin filaments is still unclear (Dalle-Donne et al., 2001). It has been reported that H_2O_2 induces rapid formation of focal adhesion complexes and reorganization of actin network in endothelial cells (Huot et al., 1998). In endothelial cells, H_2O_2 also causes activation of the p38 MAPK and this is followed by both activation of the MAPK-activated protein kinase-2/3 and the phosphorylation of the small heat shock protein (HSP) (Huot et al., 1998; Pearl-

Yafe et al., 2004). Oxidative stress has been shown to increase gap junction communication among astrocytes through reorganization of the actin network (Rouach et al., 2004).

In this paper, we report the effects of oxidative stress induced by H_2O_2 on plasma membrane properties, cytoskeleton arrangements and cell-cell interaction in rat astrocytes. Specifically, we quantitatively examined how H_2O_2 alters the phase properties of plasma membranes using the technique of fluorescence spectroscopy of Laurdan. We also studied the effects of H_2O_2 on actin polymerization and on the colocalization of myosin Va and F-actin by confocal immunofluorescence microscopy. Finally, we demonstrated that these oxidative changes involved stimulation of the p38 MAPK pathway, and the p38 inhibitor SB203580 was able to block many effects of H_2O_2.

Materials and Methods

Chemicals

Stock solutions of 1-stearoyl-2-oleoyl-*sn*-glycero-3-phosphocholine (SOPC), 1,2-dimyristoyl-*sn*-glycero-3-phosphocholine (DMPC) and cholesterol (Avanti Polar Lipids, Alabaster, AL, USA) were made in chloroform. Stock solution of Laurdan (Molecular Probes, Eugene, OR, USA) was made in methanol. $FeSO_4$ and H_2O_2 were from Sigma (St Louis, MO, USA). Dulbecco's modified Eagle's medium (DMEM), F12 medium, phosphate-buffered saline (PBS), Tris-buffered saline (TBS), trypsin-EDTA, streptomycin-penicillin and amphotericin B solutions were from Gibco (Gaithersburg, MD, USA). Fetal bovine serum (FBS) was from US Bio-Technologies (Parkerford, PA, USA). SB203580 was purchased from Promega (Madison, WI, USA).

Preparation of Laurdan-labeled vesicles

Lipids in rat brains were extracted according to the procedure described by Zhang and Sun (Zhang and Sun, 1995). Briefly, brain tissue was homogenized in 10 ml of PBS and 40 ml of chloroform-methanol (2:1 v/v) was added. The mixture was centrifuged at 2000 ***g*** for 10 minutes. The lower organic phase containing the lipids was filtered through a Pasteur pipette column packed with glass wool and anhydrous Na_2SO_4. The lipid extract was collected and stored at –20°C until use.

For preparation of lipid vesicles, brain lipids (or other purchased phospholipids) were redissolved in chloroform and about 0.001 mol% of Laurdan was added. The preparation of vesicles was accomplished by film rehydration and followed by evaporation of the chloroform under vacuum for 3 hours (Lee et al., 2001). Final addition of degassed PBS with minimal agitation led to spontaneous budding of vesicles off the glass wall and into suspension.

Lipid peroxidation in vesicles

Based on Fenton's reaction, H_2O_2 is converted to OH^- in the presence of Fe^{2+}. A $FeSO_4$ stock solution (8 mM) and a 30% H_2O_2 stock solution were prepared in ice-cold water and kept at 0°C to make Fenton's reagent. Lipid peroxidation was initiated by addition of Fenton's reagent (200 μM Fe^{2+} in H_2O_2) to the solution containing lipid vesicles. The vesicles were then incubated in the dark at 37°C for 2 hours prior to fluorescence spectroscopy of Laurdan. To study the effects of p38 MAPK inhibitor, Laurdan-labeled vesicles were preincubated with the inhibitor for 30 minutes before the addition of Fenton's reagent.

Cell culture

Astrocyte cultures were obtained from newborn rats using a standard stratification/cell shaking procedure (McCarthy and de Vellis, 1980). This procedure yielded confluent mixed glial cultures within 7-9 days, after which the flasks were shaken at 200 r.p.m. at room temperature for 4 hours to remove microglial cells. These astrocytes (>95% as quantified by anti-glial fibrillary acidic protein labeling) were subsequently subcultured onto coverslips coated with poly-D-lysine (0.4 mg/ml), and fed every 48 hours with fresh DMEM culture medium and 10% FBS. Cells were maintained at 37°C in a 5% CO_2 humidified incubator.

Cell treatment and labeling with Laurdan

After subculturing, astrocytes were grown to approximately 60% confluency. Before the addition of H_2O_2, astrocytes were incubated in a serum-free medium containing DMEM:F12 (1:1 v/v) for 2-3 hours. In the study of the role of the MAPK pathway, cells were pre-treated with different concentrations of SB203580 for 30 minutes prior to the addition of H_2O_2. After incubation of astrocytes with H_2O_2 for 2 hours at 37°C, cells were washed twice with PBS and incubated with DMEM containing 1% Laurdan for 15 minutes. Excess Laurdan was removed by washing cells three times with PBS.

Fluorescence spectroscopy with Laurdan

Spectroscopic measurements were performed at 37°C on a temperature controlled FP-750 spectrofluorometer (Jasco, Japan). Lipid vesicles were diluted in PBS and incubated for 2 hours in the presence or absence of H_2O_2 before measurement. A coverslip with attached astrocytes was put into the cuvette in Krebs-Ringer Hepes buffer (pH 7.4), and was positioned at 45° with respect to both excitation and emission ports of the fluorometer. Calculations for the generalized polarization (GP) of Laurdan followed the definition (Parasassi et al., 1990): $GP=(I_B–I_R)/(I_B+I_R)$, where I_B and I_R are the intensities at 440 nm and 490 nm, respectively, with fixed excitation wavelength of 350 nm.

Western blot analysis

Astrocytes were cultured in 60 mm dishes until 90% confluent for western blot analysis. After treatment with test agents (i.e. H_2O_2 and/or SB203580) for 30 minutes, protein lysates were prepared by adding 200 μl 1× sodium dodecyl sulfate (SDS) sample buffer (Cell Signaling Technology, Beverly, MA, USA), sonicated for 10-15 seconds to shear the DNA and reduce sample viscosity, and then boiled for 5 minutes. Protein concentration of each sample was assayed by the Bradford method. After adjusting for proteins (Bradford, 1976), aliquots were applied to a 10% SDS-polyacrylamide gel (PAGE; BioRad, Hercules, CA, USA) and blotted to nitrocellulose membrane. The sample was blocked with 5% nonfat milk, 0.1% Tween 20-PBS, pH 7.4, for 1 hour. The membrane was incubated at 4°C overnight with primary polyclonal antibodies (1:1000 dilution) against p38 MAPK and phospho-p38 MAPK (Cell Signaling Technology, Beverly, MA, USA) containing 1× TBS, 5% BSA and 0.1% Tween 20 with gentle shaking. Then the membrane was washed three times with 0.1% Tween 20-PBS for 5 minutes and incubated for 1 hour with diluted (1:1000) secondary horseradish-conjugated goat anti-rabbit IgG (Santa Cruz Biotechnology, Santa Cruz, CA, USA) at room temperature. The membrane was then washed as described above and visualized on Iso-Max imaging film (SciMart, St Louis, MO, USA) using the Lumi GLO chemiluminescence reagent.

Immunofluorescence staining for F-actin and myosin

Cells were fixed using 4% paraformaldehyde solution and permeabilized by 0.1% Triton X-100 in PBS before staining. 5% normal goat serum (NGS) in PBS was applied to the cells for 30

minutes to block non-specific binding. F-actin was fluorescently labeled with Oregon Green-phalloidin (250 nM) (Sigma, St Louis, MO, USA). To label myosin in the cells, rabbit polyclonal anti-myosin Va was added at the final concentration of 0.8 μg/ml (Chemicon, Temecula, CA, USA). This was followed by labeling with secondary antibody, Alexa Fluor®-594 donkey anti-rabbit IgG (Molecular Probes, Eugene, OR, USA) at a final concentration of 2 μg/ml.

Microscopy

Bright-field illumination and fluorescence microscopy were performed with a Nikon TE-2000 U fluorescence microscope and a 40×, NA 0.95 objective. Image were acquired using a cooled CCD camera controlled with a computer that ran a MetaVue imaging software (Universal Imaging, PA, USA). Fluorescence excitation source was controlled with a Uni-Blitz mechanical shutter.

To analyze the colocalization between myosin and F-actin, high-resolution immunofluorescence microscopy was performed with a BioRad Radiance 2000 (Carl Zeiss Microimaging, NY, USA) confocal system coupled to an Olympus IX70 (Tokyo, Japan) inverted microscope. Confocal images were acquired with a 60× NA 1.2 water immersion objective. Background was subtracted for all images prior to analysis.

Quantitative analysis of microscopic images

Actin polymerization was quantified by integrating the intensity of Oregon Green-phalloidin-labeled F-actin over the cell body. The integrated intensity was then normalized by the integrated intensity of the labeled F-actin in control cells (i.e. without H_2O_2 treatment). In this manner, the normalized intensity of cells greater than one is used to indicate that actin polymerization is enhanced compared to the control.

Relative percentages of astrocytic connections in cultures were measured by the ratio of the number of cells with TNT-like connections to the total number of cells in the image field.

The colocalization of F-actin and myosin was quantified by normalizing the area of coincident intensity to the area of noncoincident intensities.

Statistical analysis

Data are presented as mean ± s.d. from at least three independent experiments. Comparisons between groups were made with one-way ANOVA followed by Bonferroni posttests. Values of $P<0.05$ are considered statistically significant.

Results

Laurdan preferentially partitioned into vesicle bilayer membrane and cell plasma membrane

We applied the fluorescence spectroscopy of Laurdan integrated into plasma membranes of primary astrocytes and membranes of artificial lipid vesicles to study the possible changes in membrane phase properties resulting from oxidative stress produced by H_2O_2 in the presence of Fe^{2+} (Fenton's reaction). Consistent with Laurdan being an extremely hydrophobic molecule, Fig. 1A shows that this molecule preferentially partitioned into the bilayer membranes of vesicles made from rat brain lipid extract. Data in Fig. 1B show that Laurdan integrates into the plasma membranes of astrocytes. To further prove that Laurdan only partitions into plasma membranes of cells, spherical erythroblasts and neuroblastoma SH-SY5Y cells were stained with Laurdan. In fluorescence images edge-brightness of these Laurdan-labeled cells shows that Laurdan preferentially integrates into plasma membranes (Fig. S1 in supplementary material). Owing to the hydrophobic properties of Laurdan, it is reasonable that once it is integrated into the plasma membranes of astrocytes, it would be unlikely to diffuse further into the intracellular organelles. Therefore, the spectral changes of Laurdan integrated in the plasma membranes can be used as an indicator of the changes in membrane phase properties.

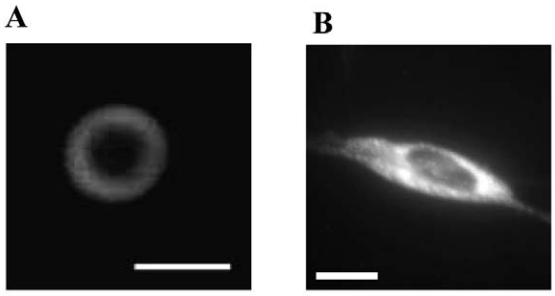

Fig. 1. Fluorescence images of Laurdan incorporated into bilayer membranes. (A) The edge-brightness of the vesicle made from rat brain lipids indicates that Laurdan preferentially partitioned into the membrane. This is consistent with Laurdan being an extremely water-insoluble molecule. (B) Laurdan incorporated into the plasma membranes of astrocytes. Scale bars: 20 μm.

H_2O_2 stimulates p38 MAPK in astrocytes

Oxidative stress has been reported to stimulate signaling pathways including the mitogen-activated protein kinases (MAPK) (Choi et al., 2004; Huot et al., 1998; Kurata, 2000; Rosenberger et al., 2001; Song et al., 2002; Usatyuk et al., 2003). In this study, western blot analysis was used to demonstrate that H_2O_2 triggers the p38 MAPK pathway in astrocytes and phosphorylation of p38 MAPK increased with increasing dose of H_2O_2 (Fig. 2A). SB203580 (at 20-30 μM), a specific inhibitor for the p38 MAPK, was capable of suppressing the phosphorylation of p38 MAPK induced by H_2O_2 (Fig. 2B). Therefore, 20 μM SB203580 was found to be the optimal concentration, and was used to study whether H_2O_2 induced MAPK pathway mediates the changes in morphology, membrane phase properties and cytoskeletal organization in astrocytes.

H_2O_2 alters membrane phase properties of astrocytes and lipid vesicles

We applied the fluorescence spectroscopy of Laurdan integrated into plasma membranes of primary astrocytes and membranes of artificial lipid vesicles to study the possible changes in membrane phase properties resulting from oxidative stress produced by H_2O_2 in the presence of Fe^{2+} (Fenton's reaction). Laurdan possesses both an electron donor and an electron receptor, so that fluorescent excitation induces a large excited-state dipole. This strong dipole tends to locally align the surrounding molecules (e.g. water), which dissipates a small fraction of the excited state energy and produces a red shift of the emission spectrum. A membrane with a lower interfacial tension (i.e. liquid crystalline phase) allows more water molecules to partition

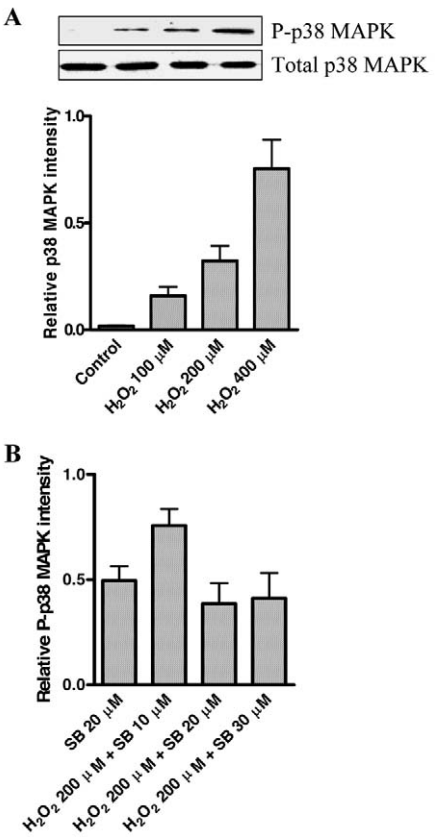

Fig. 2. Western blot analysis of p38 MAPK. (A) Western blot analysis showing that H_2O_2 increased phosphorylation of p38 MAPK in astrocytes in a dose-dependent manner (P<0.02). (B) SB203580 suppresses H_2O_2-induced phosphorylation of p38 MAPK (P<0.05). For each sample, the relative intensity of phosphorylated p38 MAPK was normalized to the total p38 MAPK. Values are the mean of three experiments.

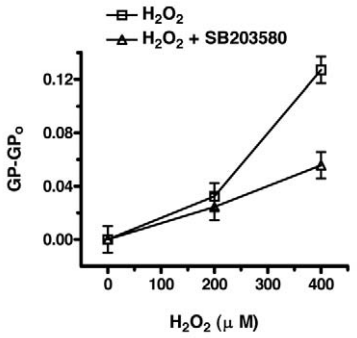

Fig. 3. The GP-GP_o values of Laurdan in astrocyte membranes at 37°C. The GP-GP_o (GP_o is the GP of control sample without H_2O_2 treatment) increased with increasing concentration of H_2O_2 (2 hours treatment) (P<0.05), indicating that the plasma membranes became more gel-like. Pretreating astrocytes with the p38 MAPK inhibitor SB203580 (20 μM, 30 minutes) reduced the change in phase properties resulting from oxidative stress (P<0.05). Values are the mean ± s.d. of three independent experiments.

into the membrane core, thus shifting Laurdan's emission maximum further into the red (Lee et al., 2001; Parasassi et al., 1990). To quantify this shift, Gratton and co-workers

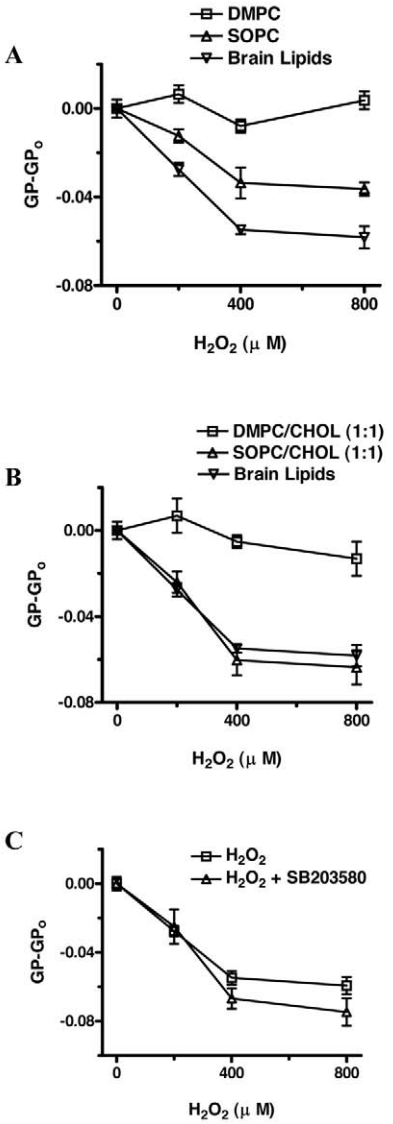

Fig. 4. The GP-GP_o values of Laurdan in model membranes at 37°C. (A) GP-GP_o of Laurdan in membranes of DMPC, SOPC and rat brain lipids. The GP-GP_o values of lipid membranes except those of DMPC membranes decreased with increasing dose of H_2O_2 (2 hours treatment) (P<0.05), indicating that the vesicle membranes became more liquid crystalline-like. (B) The effect of H_2O_2 treatment at 37°C on GP-GP_o values of Laurdan integrated in membranes composed of lipids and cholesterol. (C) GP-GP_o values of Laurdan in brain lipid vesicles pretreated with the p38 MAPK inhibitor SB203580. SB203580 (20 μM, 30 minutes) did not protect artificial brain vesicles from a phase change. Values are the mean ± s.d. of three independent experiments.

(Parasassi et al., 1990) have defined the generalized polarization (GP) and applied it to phase transitions of different lipid systems (Parasassi et al., 1991; Parasassi et al., 1993; Parasassi et al., 1994) as well as natural membranes (Parasassi et al., 1992; Waschuk et al., 2001). A higher GP value indicates that the membrane becomes more gel-like, and a lower GP indicates that the membrane becomes more liquid crystalline-like.

In our data analysis, we plotted GP-GP_o, where GP_o is the

GP of control experiments (i.e. concentration of H_2O_2 is zero). Therefore, GP-GP_o of the control is always zero, serving as a common reference datum. We found that the GP-GP_o of Laurdan in astrocyte membranes was increased by increasing dose of H_2O_2 (Fig. 3), suggesting that H_2O_2 causes astrocyte membranes to become more gel-like. These effects of H_2O_2 on astrocyte membranes could be suppressed by the MAPK inhibitor, SB203580 (Fig. 3).

In order to rule out the cellular complexity in astrocytes, and to reveal the effects of ROS induced by H_2O_2 on bilayer membranes through direct oxidation, we also measured the GP-GP_o values for membrane vesicles made from (a) rat brain lipid extract, (b) DMPC, a symmetric saturated phospholipid, and (c) SOPC, an asymmetric unsaturated phospholipid, which were incubated with Fenton's reagent. Contrary to the results from astrocyte membranes, the GP-GP_o values of Laurdan in membranes of brain lipid vesicles and SOPC decreased (i.e. becoming more liquid crystalline-like) with increasing doses of H_2O_2, whereas that in membranes of DMPC remained almost zero or unchanged (Fig. 4A). Such decreases in GP-GP_o values of Laurdan in membranes of brain lipid vesicles and SOPC were observed only in the presence of Fe^{2+} (data not shown). These results suggest that ROS generated by H_2O_2 reacts with unsaturated acyl chains, and produces more asymmetric phospholipids, thereby loosening the molecular packing in the hydrophobic core of the lipid bilayer. Subsequently, membranes made of brain lipids and SOPC became more liquid crystalline-like with increasing H_2O_2.

In addition to unsaturated phospholipids, cholesterol is another major lipid component in astrocyte membranes. However, we did not observe significant effects of H_2O_2 on the phase properties of membranes made of cholesterol/DMPC (1:1) (Fig. 4B). Therefore, GP-GP_o values of cholesterol/SOPC membranes were smaller than those of SOPC membranes, which was due to different compositions of the two membrane systems and not to the oxidation of cholesterol (Fig. 4B). SB203580 did not reduce membrane phase change induced by H_2O_2 in vesicle bilayer membranes (Fig. 4C). Since the reactions of ROS with unsaturated phospholipids cause the lipid bilayer membranes to become more liquid crystalline-like, whereas the plasma membranes of astrocytes become more gel-like, this would suggest that changes in the phase properties of plasma membranes of astrocytes during oxidative insults are not simply due to direct oxidation of phospholipids and cholesterol.

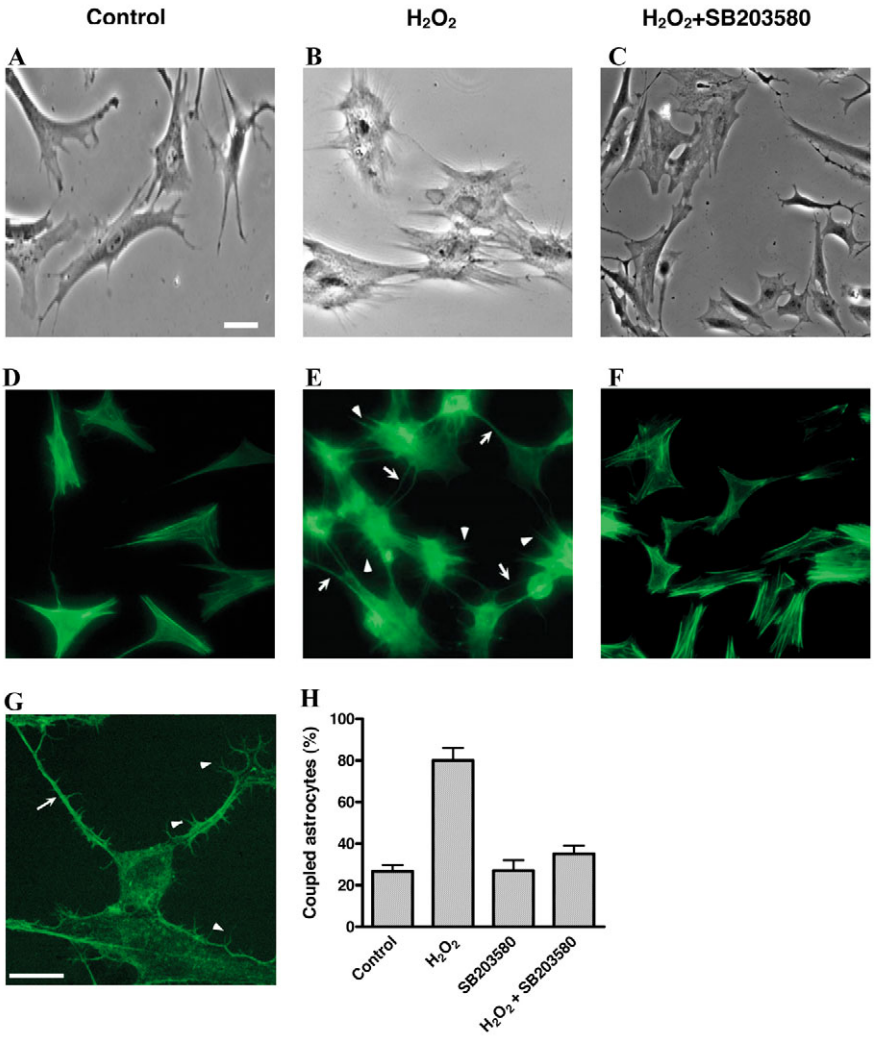

Fig. 5. H_2O_2 increased cytonemes and TNT-like connections in astrocytes. (A-C) Phase contrast microscopy shows morphological changes of astrocytes. (D-G) Immunofluorescence images of Oregon Green-phalloidin-labeled F-actin astrocytes. (A,D) Untreated control; (B,E,G) treated with H_2O_2 (200 μM, 2 hours); (C,F) treated with H_2O_2 (200 μM, 2 hours) and SB203580 (20 μM, 30 minutes). (G) High magnification confocal micrograph shows the formation of TNT-like connections (arrow) and cytonemes (arrowheads). (H) The percentage of cells having TNT-like connections with other cells. The relative percentages of astrocytic connections in cultures was calculated as the ratio of the number of cells with TNT-like connections to the total number of cells in the same image. Each value is the average from at least 120 cells from three independent experiments. Treatment with H_2O_2 (200 μM, 2 hours) significantly increased the formation of TNT-like connections (P<0.01), and pre-treatment with SB203580 (20 μM, 30 minutes) significantly counteracted the formation of TNT-like connections (P<0.01). Scale bars: 20 μm in A, and 5 μm in G.

H_2O_2 increases formation of cytonemes and nanotubes and promotes actin polymerization in astrocytes

Besides the effects on plasma membranes, oxidative stress is known to cause cytoskeletal reorganizations in cells (Qian et al., 2003; Rosado et al., 2002; Rouach et al., 2004; Zhao and Davis, 1998). Fig. 5E,G shows the effects of oxidative stress on the formation of actin-enriched protrusions (white arrowheads), similar to cytonemes described by Ramirez-Weber and Kornberg (Ramirez-Weber and Kornberg, 1999), and the formation of tunneling nanotube (TNT)-like connections (white arrows)

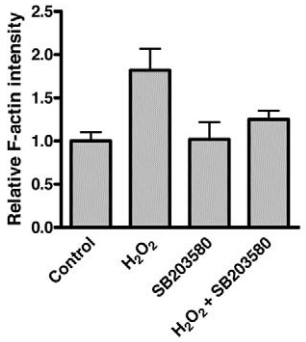

Fig. 6. H_2O_2 promoted actin polymerization in astrocytes. The relative intensity of fluorescently labeled F-actin in astrocytes was calculated from the integrated fluorescent intensities per astrocyte normalized to those without H_2O_2 treatment. Each data point represents an average value obtained from at least 150 cells from three independent experiments. Treatment with H_2O_2 (200 μM, 2 hours) increased the polymerization of actin by up to 180% in astrocytes (P<0.01), and pretreatment of cells with SB203580 (20 μM, 30 minutes) suppressed this effect induced by H_2O_2 (P<0.01).

similar to the TNT described by Rustom et al. (Rustom et al., 2004). These structures are F-actin-enriched (Fig. 5E), and contain myosin (Fig. 7J). TNT-like connections and cytonemes were observed only on solid surfaces supporting cell cultures of astrocytes. After treatment with H_2O_2, astrocytes tend to establish connections with each other, resulting in a significant increase (P<0.01) in the number of actin filament-enriched TNT-like structures (Fig. 5H). Such reorganization of F-actin in astrocytes after H_2O_2 treatment is dramatic when compared with non-treated astrocytes, in which the actin stress fibers spread out evenly, forming a few cell motility structures (e.g. rosette-like dots) at the cell leading edges and within the cell bodies.

Enhanced actin polymerization may be a part of the process in the formations of cytonemes and TNT-like connections in astrocytes under oxidative stress. Therefore, we quantified the fluorescence intensity of Oregon Green-phalloidin-labeled F-actin in astrocytes. The intensity of fluorescence in astrocytes treated with H_2O_2 was significantly increased (P<0.01) as compared to that without H_2O_2 treatment (Fig. 6).

In addition, SB203580 was found to suppress the enhanced formation of actin-enriched structures, cytonemes and nanotubes (Fig. 5C,F,H), and the polymerization of actin induced by H_2O_2 (Fig. 6).

H_2O_2 enhances colocalization of myosin with actin filaments in astrocytes

Myosin is an actin-associated motor protein, and is known to play an important role in cellular transportation and communication. Since H_2O_2 enhances actin polymerization and induces F-actin reorganization, it may also alter the colocalization of myosin to F-actin. We quantified the effect of H_2O_2 on the colocalization of myosin with F-actin by analyzing confocal images of fluorescently labeled actin and myosin in astrocytes. Fig. 7 shows images of fluorescently labeled actin, myosin and the colocalization images used for quantitative analysis. Our results indicated a significant increase in colocalization of myosin Va with F-actin after H_2O_2 treatment in astrocytes, while pre-treatment with SB203580 could partially reduce this enhanced colocalization induced by H_2O_2 (Fig. 7K). Myosin Va was also observed inside the TNT-like connections (Fig. 7J).

Discussion

In this study, we examined the effects of oxidative stress on astrocyte membranes and the cytoskeleton by exposing astrocytes to H_2O_2, an oxidant commonly used to examine oxidative mechanisms mediating cell death (Misonou et al., 2000). A study by Hyslop et al. (Hyslop et al., 1995) reported that under ischemic conditions, the concentration of H_2O_2 in the rat striatum can possibly reach 200 μM. In our study, we observed astrocyte membrane phase properties and the phosphorylation of p38 MAPK at concentrations of H_2O_2 ranging from 0 to 400 μM and we chose to use 200 μM to study morphological changes and for observation and quantification of changes in actin and myosin using immunofluorescence.

Since Fe^{2+} is present in the cell culture medium and inside astrocytes, addition of H_2O_2 alone to the cell culture is sufficient to initiate Fenton's reaction. Results of this study demonstrate that oxidative stress induced by H_2O_2 decreases astrocyte membrane fluidity, induces cytoskeletal reorganization, and increase the formation of cytonemes and TNT-like connections. In addition, the p38 MAPK inhibitor, SB203580, could suppress these effects produced by H_2O_2. As oxidative stress is involved in a number of neurodegenerative diseases, this study, aimed at understanding the effects of H_2O_2 on astrocytes, should prove relevant and significant.

In order to investigate the origins of the effects of H_2O_2 on astrocyte membranes, we systematically characterized phase properties of astrocyte membranes and compared them to vesicles made from (a) brain lipid extract, (b) unsaturated phospholipids (SOPC), (c) symmetric saturated phospholipids (DMPC), (d) cholesterol/SOPC (1:1) and (e) cholesterol/DMPC (1:1). Total brain lipid extract is composed of acidic and neutral phospholipids, gangliosides, cholesterol, sphingolipids and isoprenoids (McLaurin et al., 2002). Thus, vesicles derived from brain lipids serve as a simple model system to mimic astrocyte membranes without any complications produced by cellular processes. Our results show that increasing doses of H_2O_2 cause membranes of brain lipid vesicles to become more liquid crystalline-like (Fig. 4) but membranes of astrocytes to become more gel-like (Fig. 3). Since the results from brain lipid vesicles represent the direct effects of lipid peroxidation, the contrasting results between membranes of brain lipid vesicles and plasma membranes of astrocytes suggest that the effects of H_2O_2 on astrocyte membranes are not simply due to lipid peroxidation, but also to alterations of cell membrane proteins and organization of intracellular structures. Clearly, more studies are needed to explore how oxidative stress alters cell membrane structures through intracellular signaling pathways.

We also examined the effects of oxidative stress on the F-actin fibers in astrocytes. Actin filaments are involved in a wide variety of cellular processes, including cell motility, cell cycle control, cellular structure and cell signaling. They function in cellular processes by undergoing dynamic structural reorganization or remodeling, leading to the formation of discrete structures at the periphery for attachment to the

substratum in response to different signals. In this study, we found that H_2O_2 increases polymerization of actin and the formation of cellular protrusions (cytonemes), and TNT-like connections in primary rat astrocytes. These results are consistent with studies in other cell types indicating a rapid remodeling of the structure of actin filaments upon oxidative stress (Qian et al., 2003; Zhao and Davis, 1998). However, there is also evidence that oxidation of actin by strong oxidant compounds may disrupt the actin network in cells (Dalle-Donne et al., 2002; Valen et al., 1999), leading to inhibition of actin polymerization and actin filament depolymerization. Our data indicate that oxidative stress significantly enhances the formation of intercellular TNT-like connections and the association of myosin to actin filaments. Rustom and his coworkers (Rustom et al., 2004) regarded TNT as an independent form of mammalian cell-cell communication. These TNTs are F-actin-enriched structures, and can transport organelles from one cell to another. It is a highly coordinated process regulated by cell signaling cascades. In astrocytes, oxidative stress is known to cause the formation of gap junction, which is another form of intercellular connection (Rouach et al., 2004). With the notion of TNTs functioning as transportation highways (Rustom et al., 2004), our results lead to the hypothesis that oxidative stress enhances communication between astrocytes. Therefore, our results lay the groundwork to study the possible communication among astrocytes altered by oxidative stress.

Our findings suggest that changes in actin polymerization are not caused by direct oxidation of actin by H_2O_2, but may involve signaling pathways. Indeed, oxidative stress is known to induce signaling cascades and subsequent cytoskeletal remodeling in a number of neural and non-neural cell systems (Bundy et al., 2005; Carvalho et al., 2004; Choi et al., 2004; Huot et al., 1998; Kevil et al., 2001; Kurata, 2000; Usatyuk and Natarajan, 2004; Usatyuk et al., 2003). In dopaminergic neurons, phosphorylation of p38 MAPK by oxidative stress is

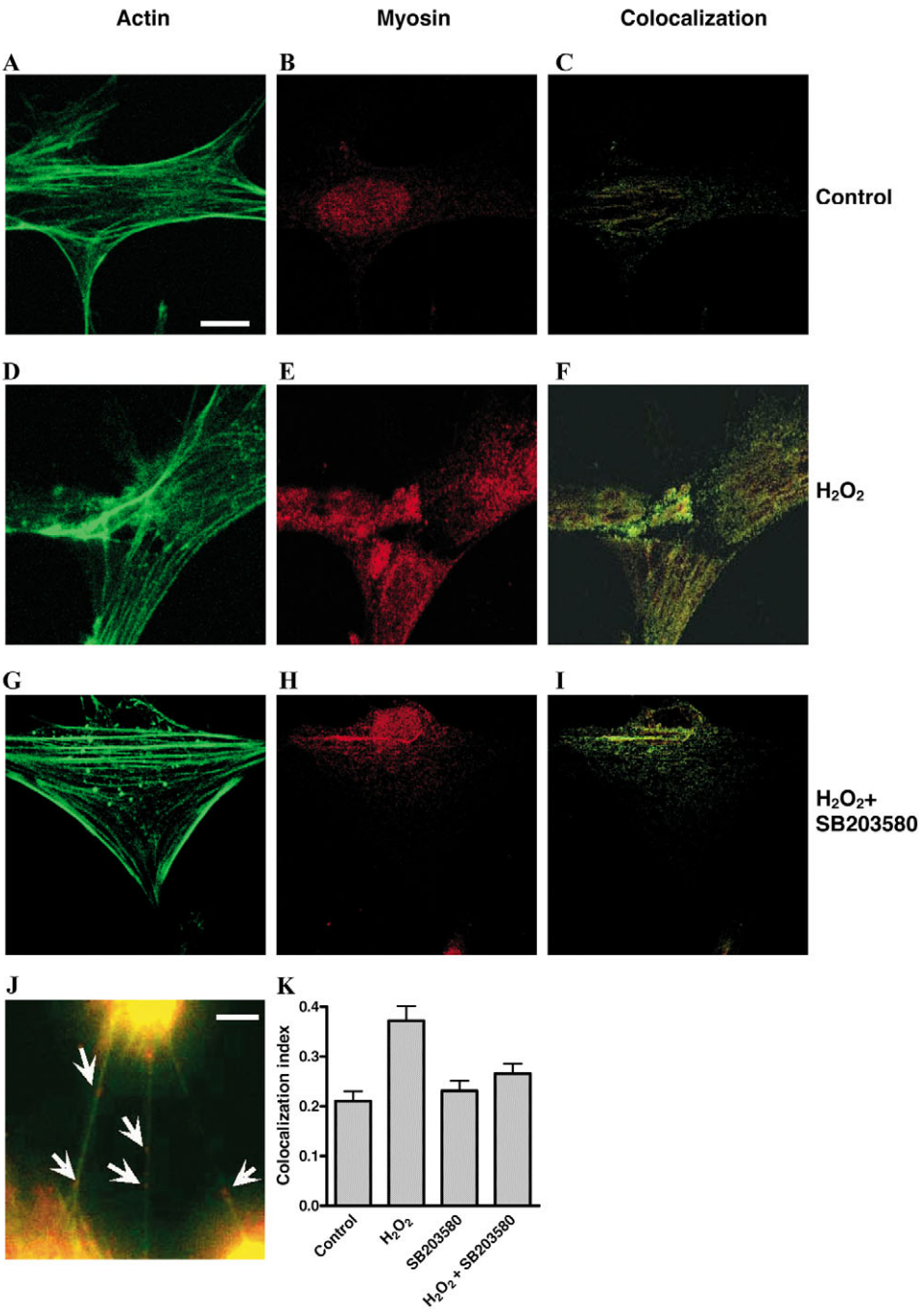

Fig. 7. H_2O_2 promoted colocalization of myosin with the actin network in astrocytes. (A,D,G) F-actin labeled with Oregon Green. (B,E,H) Myosin Va labeled with Texas Red. (C,F,I) Colocalization of F-actin and myosin Va. (A-C) Control cells; (D-F) cells treated with H_2O_2 (200 μM, 2 hours); (G-I) cells treated with H_2O_2 (200 μM, 2 hours) and SB203580 (20 μM, 30 minutes). The images in C, F and I were obtained by suppressing all colors except yellow in Adobe Photoshop. (J) Myosin present inside the actin-enriched TNT-like connections. (K) The colocalization index of myosin with actin in astrocytes. The index is the area of coincident intensity (yellow in C,F,I) normalized by the area of noncoincident intensities (green + red – yellow). Each data point represents an average value obtained from at least 150 cells from three independent experiments. Treatment with H_2O_2 (200 μM, 2 hours) increased colocalization of myosin Va with actin (P<0.01), and pretreatment of cells with SB203580 (20 μM, 30 minutes) reduced this colocalization (P<0.01). Scale bars: 15 μm in A, 10 μm in J.

linked to activation of caspases and apoptotic pathways (Choi et al., 2004) and p38 MAPK mediates the formation of actin stress fibers induced by β-amyloid peptide (Song et al., 2002). Our study, with primary rat astrocytes, demonstrated a dose-dependent increase in phosphorylation of p38 MAPK upon treatment with H_2O_2, and inhibition of p38 MAPK reduced H_2O_2-mediated changes in membrane phase properties and cytoskeletal reorganization. These results suggest that oxidative stress-induced activation of MAPK is important in modulation of cytoskeletal organization as well as downstream pathways leading to the cell death mechanism.

In conclusion, results of this study demonstrate that H_2O_2 causes astrocyte membranes to become more gel-like and induces actin polymerization and, subsequently, enhances formation of cytonemes and cell-to-cell TNT-like connections. Based on these results, we suggest that oxidative stress may have an important impact on astrocyte membranes, signaling pathways and cytoskeletal arrangements. All these effects may lead to altered astrocyte functions.

This work was supported by grants DHHS 5P01 ES10535 and 1P01 AG18357 from NIH and an MU Research Board grant, URB-04-038.

References

Aksenov, M. Y., Aksenova, M. V., Butterfield, D. A., Geddes, J. W. and Markesbery, W. R. (2001). Protein oxidation in the brain in Alzheimer's disease. *Neuroscience* **103**, 373-383.

Bradford, M. M. (1976). A rapid and sensitive method for the quantitation of microgram quantities of protein utilizing the principle of protein-dye binding. *Anal. Biochem.* **72**, 248-254.

Bundy, R. E., Hoare, G. S., Kite, A., Beach, J., Yacoub, M. and Marczin, N. (2005). Redox regulation of p38 MAPK activation and expression of ICAM-1 and heme oxygenase-1 in human alveolar epithelial (A549) cells. *Antioxid. Redox Sign.* **7**, 14-24.

Butterfield, D. A. and Lauderback, C. M. (2002). Lipid peroxidation and protein oxidation in Alzheimer's disease brain: potential causes and consequences involving amyloid β-peptide-associated free radical oxidative stress. *Free Radic. Biol. Med.* **32**, 1050-1060.

Carvalho, H., Evelson, P., Sigaud, S. and Gonzalez-Flecha, B. (2004). Mitogen-activated protein kinases modulate H_2O_2-induced apoptosis in primary rat alveolar epithelial cells. *J. Cell Biochem.* **92**, 502-513.

Choi, W. S., Eom, D. S., Han, B. S., Kim, W. K., Han, B. H., Choi, E. J., Oh, T. H., Markelonis, G. J., Cho, J. W. and Oh, Y. J. (2004). Phosphorylation of p38 MAPK induced by oxidative stress is linked to activation of both caspase-8- and -9-mediated apoptotic pathways in dopaminergic neurons. *J. Biol. Chem.* **279**, 20451-20460.

Coyle, J. T. and Puttfarcken, P. (1993). Oxidative stress, glutamate, and neurodegenerative disorders. *Science* **262**, 689-695.

Dalle-Donne, I., Rossi, R., Milzani, A., Di Simplicio, P. and Colombo, R. (2001). The actin cytoskeleton response to oxidants: from small heat shock protein phosphorylation to changes in the redox state of actin itself. *Free Radic. Biol. Med.* **31**, 1624-1632.

Dalle-Donne, I., Rossi, R., Giustarini, D., Gagliano, N., Di Simplicio, P., Colombo, R. and Milzani, A. (2002). Methionine oxidation as a major cause of the functional impairment of oxidized actin. *Free Radic. Biol. Med.* **32**, 927-937.

Desagher, S., Glowinski, J. and Premont, J. (1996). Astrocytes protect neurons from hydrogen peroxide toxicity. *J. Neurosci.* **16**, 2553-2562.

Gyulkhandanyan, A. V., Feeney, C. J. and Pennefather, P. S. (2003). Modulation of mitochondrial membrane potential and reactive oxygen species production by copper in astrocytes. *J. Neurochem.* **87**, 448-460.

Howe, C. J., LaHair, M. M., McCubrey, J. A. and Franklin, R. A. (2004). Redox regulation of the CaM-kinases. *J. Biol. Chem.* **279**, 44573-44581.

Huang, X., Moir, R. D., Tanzi, R. E., Bush, A. I. and Rogers, J. T. (2004). Redox-active metals, oxidative stress, and Alzheimer's disease pathology. *Ann. New York Acad. Sci.* **1012**, 153-163.

Huot, J., Houle, F., Rousseau, S., Deschesnes, R. G., Shah, G. M. and Landry, J. (1998). SAPK2/p38-dependent F-actin reorganization regulates early membrane blebbing during stress-induced apoptosis. *J. Cell Biol.* **143**, 1361-1373.

Hyslop, P. A., Zhang, Z., Pearson, D. V. and Phebus, L. A. (1995). Measurement of striatal H_2O_2 by microdialysis following global forebrain ischemia and reperfusion in the rat: correlation with the cytotoxic potential of H_2O_2 in vitro. *Brain Res.* **671**, 181-186.

Jacobson, J. and Duchen, M. R. (2002). Mitochondrial oxidative stress and cell death in astrocytes – requirement for stored Ca^{2+} and sustained opening of the permeability transition pore. *J. Cell Sci.* **115**, 1175-1188.

Kevil, C. G., Oshima, T. and Alexander, J. S. (2001). The role of p38 MAP kinase in hydrogen peroxide mediated endothelial solute permeability. *Endothelium* **8**, 107-116.

Kurata, S. (2000). Selective activation of p38 MAPK cascade and mitotic arrest caused by low level oxidative stress. *J. Biol. Chem.* **275**, 23413-23416.

Lee, J. C. M., Law, R. J. and Discher, D. E. (2001). Bending contributions hydration of phospholipid and block copolymer membranes: Unifying correlations between probe fluorescence and vesicle thermoelasticity. *Langmuir* **17**, 3592-3597.

Lin, H. J., Wang, X., Shaffer, K. M., Sasaki, C. Y. and Ma, W. (2004). Characterization of H_2O_2-induced acute apoptosis in cultured neural stem/progenitor cells. *FEBS Lett.* **570**, 102-106.

McCarthy, K. D. and de Vellis, J. (1980). Preparation of separate astroglial and oligodendroglial cell cultures from rat cerebral tissue. *J. Cell Biol.* **85**, 890-902.

McLaurin, J., Darabie, A. A. and Morrison, M. R. (2002). Cholesterol, a modulator of membrane-associated Aβ-fibrillogenesis. *Ann. New York Acad. Sci.* **977**, 376-383.

Misonou, H., Morishima-Kawashima, M. and Ihara, Y. (2000). Oxidative stress induces intracellular accumulation of amyloid β-protein (Aβ) in human neuroblastoma cells. *Biochemistry* **39**, 6951-6959.

Parasassi, T., De Stasio, G., d'Ubaldo, A. and Gratton, E. (1990). Phase fluctuation in phospholipid membranes revealed by Laurdan fluorescence. *Biophys. J.* **57**, 1179-1186.

Parasassi, T., De Stasio, G., Ravagnan, G., Rusch, R. M. and Gratton, E. (1991). Quantitation of lipid phases in phospholipid vesicles by the generalized polarization of Laurdan fluorescence. *Biophys. J.* **60**, 179-189.

Parasassi, T., Di Stefano, M., Ravagnan, G., Sapora, O. and Gratton, E. (1992). Membrane aging during cell growth ascertained by Laurdan generalized polarization. *Exp. Cell. Res.* **202**, 432-439.

Parasassi, T., Ravagnan, G., Rusch, R. M. and Gratton, E. (1993). Modulation and dynamics of phase properties in phospholipid mixtures detected by Laurdan fluorescence. *Photochem. Photobiol.* **57**, 403-410.

Parasassi, T., Giusti, A. M., Gratton, E., Monaco, E., Raimondi, M., Ravagnan, G. and Sapora, O. (1994). Evidence for an increase in water concentration in bilayers after oxidative damage of phospholipids induced by ionizing radiation. *Int. J. Radiat. Biol.* **65**, 329-334.

Pearl-Yafe, M., Halperin, D., Scheuerman, O. and Fabian, I. (2004). The p38 pathway partially mediates caspase-3 activation induced by reactive oxygen species in Fanconi anemia C cells. *Biochem. Pharmacol.* **67**, 539-546.

Qian, Y., Luo, J., Leonard, S. S., Harris, G. K., Millecchia, L., Flynn, D. C. and Shi, X. (2003). Hydrogen peroxide formation and actin filament reorganization by Cdc42 are essential for ethanol-induced in vitro angiogenesis. *J. Biol. Chem.* **278**, 16189-16197.

Ramirez-Weber, F. A. and Kornberg, T. B. (1999). Cytonemes: cellular processes that project to the principal signaling center in *Drosophila* imaginal discs. *Cell* **97**, 599-607.

Robb, S. J. and Connor, J. R. (1998). An in vitro model for analysis of oxidative death in primary mouse astrocytes. *Brain Res.* **788**, 125-132.

Robb, S. J., Robb-Gaspers, L. D., Scaduto, R. C., Jr, Thomas, A. P. and Connor, J. R. (1999). Influence of calcium and iron on cell death and mitochondrial function in oxidatively stressed astrocytes. *J. Neurosci. Res.* **55**, 674-686.

Rosado, J. A., Gonzalez, A., Salido, G. M. and Pariente, J. A. (2002). Effects of reactive oxygen species on actin filament polymerisation and amylase secretion in mouse pancreatic acinar cells. *Cell Signal* **14**, 547-556.

Rosenberger, J., Petrovics, G. and Buzas, B. (2001). Oxidative stress induces proorphanin FQ and proenkephalin gene expression in astrocytes through p38- and ERK-MAP kinases and NF-κB. *J. Neurochem.* **79**, 35-44.

Rouach, N., Calvo, C. F., Duquennoy, H., Glowinski, J. and Giaume, C. (2004). Hydrogen peroxide increases gap junctional communication and induces astrocyte toxicity: regulation by brain macrophages. *Glia* **45**, 28-38.

Rustom, A., Saffrich, R., Markovic, I., Walther, P. and Gerdes, H. H.

(2004). Nanotubular highways for intercellular organelle transport. *Science* **303**, 1007-1010.

Shin, S. Y., Kim, C. G., Jho, E. H., Rho, M. S., Kim, Y. S., Kim, Y. H. and Lee, Y. H. (2004). Hydrogen peroxide negatively modulates Wnt signaling through downregulation of β-catenin. *Cancer Lett.* **212**, 225-231.

Song, C., Perides, G., Wang, D. and Liu, Y. F. (2002). β-Amyloid peptide induces formation of actin stress fibers through p38 mitogen-activated protein kinase. *J. Neurochem.* **83**, 828-836.

Usatyuk, P. V. and Natarajan, V. (2004). Role of mitogen-activated protein kinases in 4-hydroxy-2-nonenal-induced actin remodeling and barrier function in endothelial cells. *J. Biol. Chem.* **279**, 11789-11797.

Usatyuk, P. V., Vepa, S., Watkins, T., He, D., Parinandi, N. L. and Natarajan, V. (2003). Redox regulation of reactive oxygen species-induced p38 MAP kinase activation and barrier dysfunction in lung microvascular endothelial cells. *Antioxid. Redox Signal.* **5**, 723-730.

Valen, G., Sonden, A., Vaage, J., Malm, E. and Kjellstrom, B. T. (1999). Hydrogen peroxide induces endothelial cell atypia and cytoskeleton depolymerization. *Free Radic. Biol. Med.* **26**, 1480-1488.

van Rossum, G. S. A. T., Drummen, G. P. C., Verkleij, A. J., Post, J. A. and Boonstra, J. (2004). Activation of cytosolic phospholipase A_2 in Her14 fibroblasts by hydrogen peroxide: a $p42/44^{MAPK}$-dependent and phosphorylation-independent mechanism. *Biochim. Biophys. Acta* **1636**, 183-195.

Waschuk, S. A., Elton, E. A., Darabie, A. A., Fraser, P. E. and McLaurin, J. A. (2001). Cellular membrane composition defines Aβ-lipid interactions. *J. Biol. Chem.* **276**, 33561-33568.

Zhang, J. P. and Sun, G. Y. (1995). Free fatty acids, neutral glycerides, and phosphoglycerides in transient focal cerebral ischemia. *J. Neurochem.* **64**, 1688-1695.

Zhao, Y. and Davis, H. W. (1998). Hydrogen peroxide-induced cytoskeletal rearrangement in cultured pulmonary endothelial cells. *J. Cell. Physiol.* **174**, 370-379.